

Supporting Information

SI 1. Bending tests

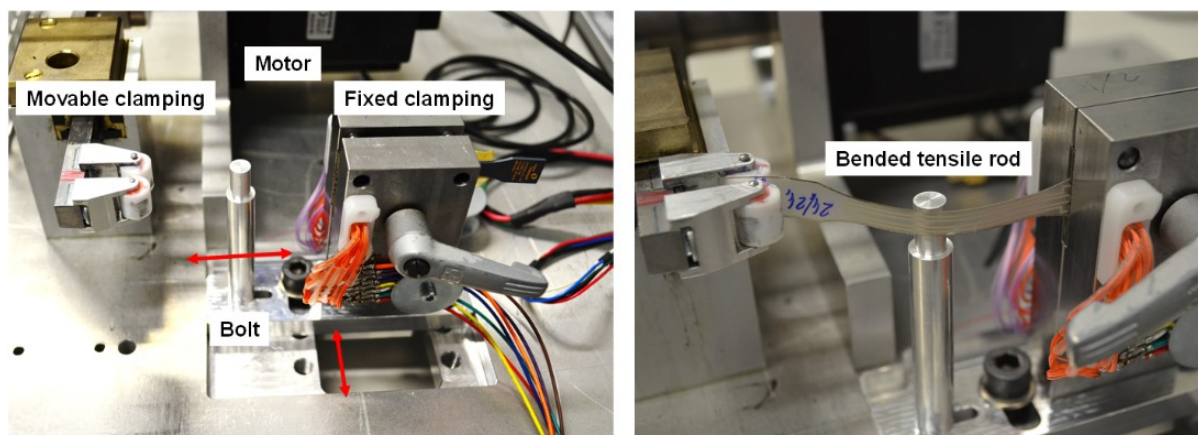


Figure S1. Bending test rig. The electrical measurement is performed using the fixed clamps. The movable specimen clamps allow a deflection of 24 mm. The movable bolt was adjusted to three different positions to vary the strain on the printed conductors.

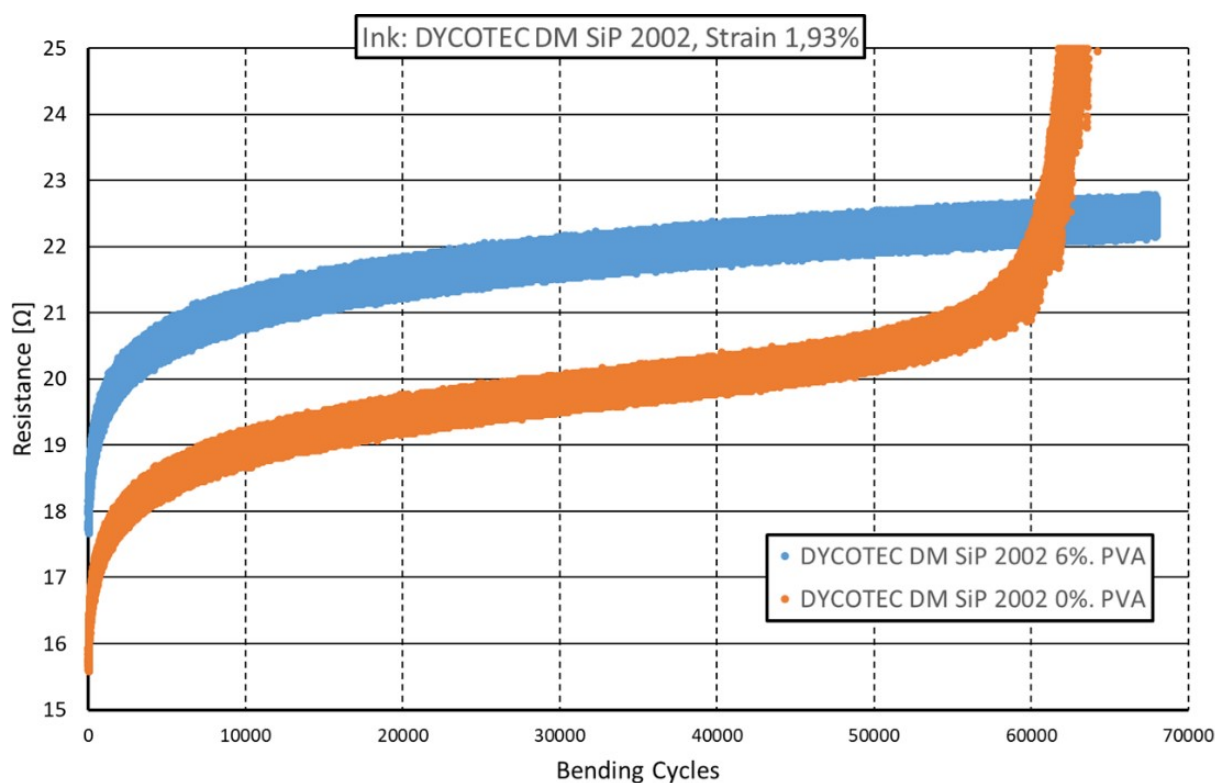


Figure S2 Electrical resistance during bending. Increase of resistance in a screen-printed conductor during cyclic bending tests for samples with and without underlying PVA.

SI 2. Evaluation of bending test results

Figure S3 displays exemplary Weibull distributions. On the left, it is evident that as the strain increases, the lifetime decreases significantly. The curve on the right shows that the PVA layer positively influences the lifetime under bending stress. It can be assumed that the PVA layer reduces the stresses induced by bending in the conductive tracks, effectively serving as a compensation layer.

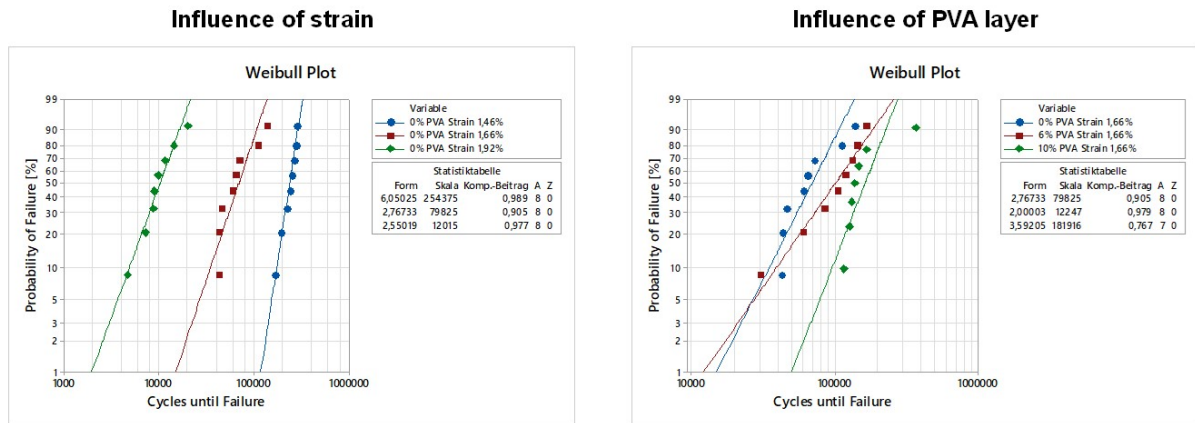


Figure S3. Weibull distributions. Probability of failure vs cycles until failure of DM SIP 2002 (Dycotec) screen printing paste on PC in dependence on the applied strain (left) and presence of an underlying PVA layer at 1.66% stain (right).

The statistical analysis of failures using Weibull distributions was conducted using the statistical software Minitab® (Version 18). The failure criterion was a 20% increase in resistance from the initial value. To assess and compare the reliability of printed conductive tracks, including the PVA layer, S-N (Wöhler) curves were determined. The procedural steps are illustrated in Figure S4.

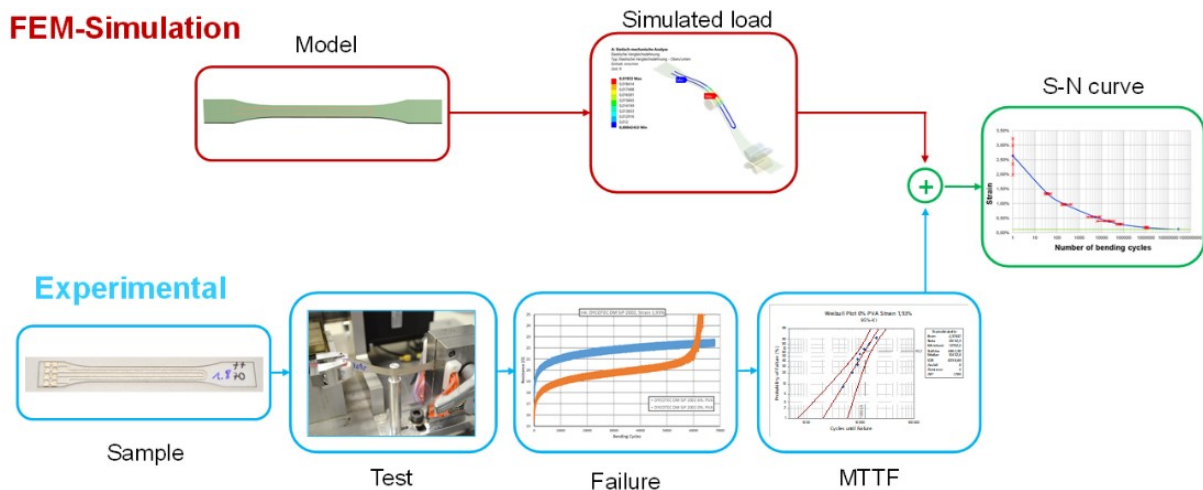


Figure S4. S-N curves. Procedural steps to determine S-N curves (Wöhler curves).

SI 3. Geometrical design

The objective of this structure is to be able to test release layer and conductive ink prints after thermoforming and overmoulding processes. The advantage of IME vs classical electronics is that it allows to integrate circuitry inside the housing walls and other more complex shapes than flat PCB. That implies deformations of the printed tracks during the whole process and especially during the thermoforming. The design of the 'meander structure' is given in the following figure.

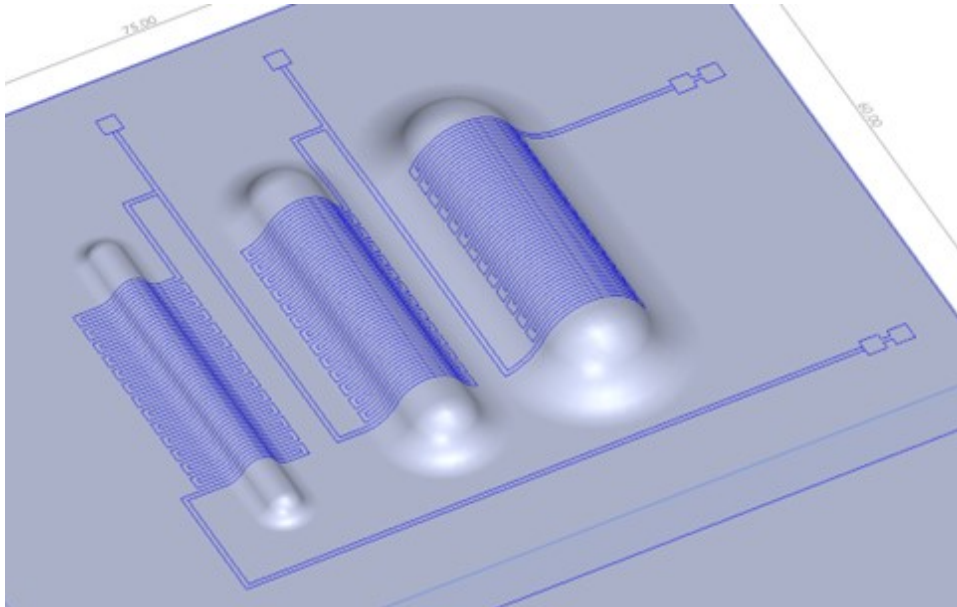


Figure S5. Design of the meander structure.

This structure includes a 500 μm wide track that runs through three zones with radii of curvature different from 2, 4 and 6 mm. Each structure has a length of about 440 mm and the whole design 1500 mm. When thermoforming the sheet after printing, the conductive tracks will be bent and stretched according to these curvatures. The objective is to see the impact of each curvature on the residual electrical conduction of the tracks and to see the influence of the PVA layer on these results. Different connection areas were put between each structure to localize more easily the eventual failures.

SI 4. Electrical resistance measurements

Table S1. Resistance of bending test samples. Track thicknesses and resistances (outer U-shape track) of screen-printed pastes.

Substrate	Coating	Paste	Thickness	Resistance
			μm	Ohm
PC	no	Bectron CP6680	~24	6
PC	no	CM 112-15A	~25	9,6
PC	no	DYC DM SIP 2002	~9	18
PC	6% PVA	Bectron CP6680	~17	7
PC	6% PVA	CM 112-15A	~14	10,7
PC	6% PVA	DYC DM SIP 2002	~9	16,8
PC	10% PVA	Bectron CP6680	~23	5,7
PC	10% PVA	CM 112-15A	~11	10,5
PC	10% PVA	DYC DM SIP 2002	~16	16,7

Table S2. Resistance of meander structures. Electrical resistances measured for the longest track before and after the thermoforming process using meander structures. The three structures of the meander were deformed respectively with a radius of curvature of 2, 4 and 6 mm.

				Flat sheets		Thermoformed sheets
Substrate	Paste	Substrate Coating	Substrate side	Resistance	Track Thickness	Resistance
				Ohm	μm	Ohm
PC LEXAN 8B35	CM 112-15A	NO (rough side)		350	-	-
				300		2380
				290		5800
				287		-
				304		-
			Avg	306.2		4090
		Std dev	25.5	2418.3		
		PVA 6%	smooth side	241		335
			rough side	231		354
			smooth side	256		271
			smooth side	190		173
			smooth side	198		233
	smooth side		229	-		
	Avg	224.2	273.2			
	Std dev	25.4	74.2			
	Bectron CP6680	NO (rough side)		64.5	~10 μm (ink buried in the substrate roughness)	59.3
				66		78.7
				64		67.3
				64		61.2
				67		69.8
			Avg	65.1		67.3
		Std dev	1.3	7.7		
		PVA 6%	smooth side	79		-
			rough side	82.7		-
rough side			78,9	-		
rough side			78,8	-		

		rough side	80.7		-
		rough side	67.2		-
		rough side	68.1		-
		Avg	76.5		-
		Std dev	6.2		-
DM SIP-2002	NO (rough side)		266	-	239
			291	-	307
			276	-	265
			276	-	240
			274	-	263
		Avg	276.6	-	262.8
		Std dev	9.0	-	27.6
	PVA 6%	smooth side	288	-	311
		smooth side	288	-	417
		smooth side	292	-	370
		smooth side	290	-	311
		rough side	266	-	374
		smooth side	294	-	262
		Avg	286.3	-	340.8
Std dev		10.2	-	56.1	

SI 5. Setups and fracture behavior in the adhesion tests

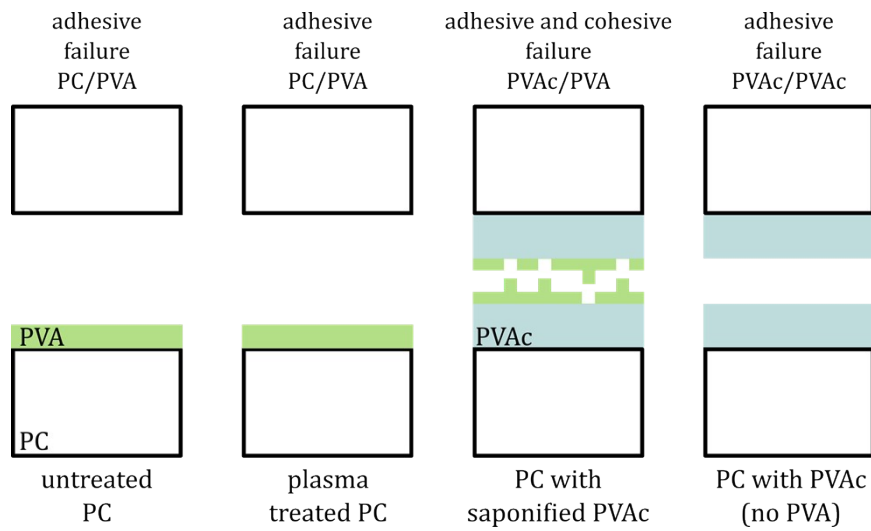


Figure S6. Setups and fracture behavior in the adhesion tests. Photograph of 13% PVA printed on PC, with (left) and without (right) plasma treatment.

SI 6. Bubble formation during screen printing of PVA

Screen printing of PVA on PC leads to dewetting effects without plasma pretreatment as shown in Figure S7.

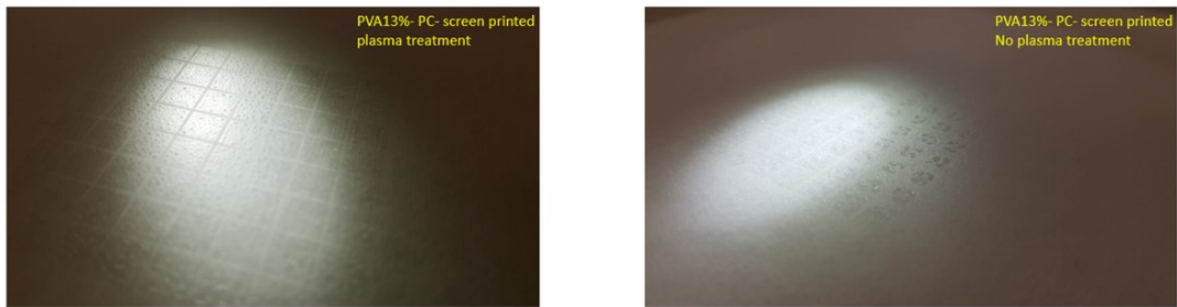


Figure S7. Dewetting of screen-printed PVA on PC. Photograph of 13% PVA printed on PC, with (left) and without (right) plasma treatment.

Bubble formation occurs during printing. Since the solutions were degassed adequately before printing, air was entrained solely by the screen printing process.

The deposit thickness was insufficient to exceed the roughness level of the PC substrate ($Ra \approx 1 \mu\text{m}$).

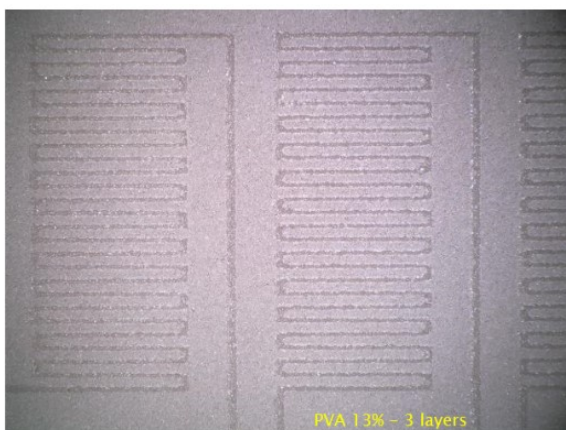
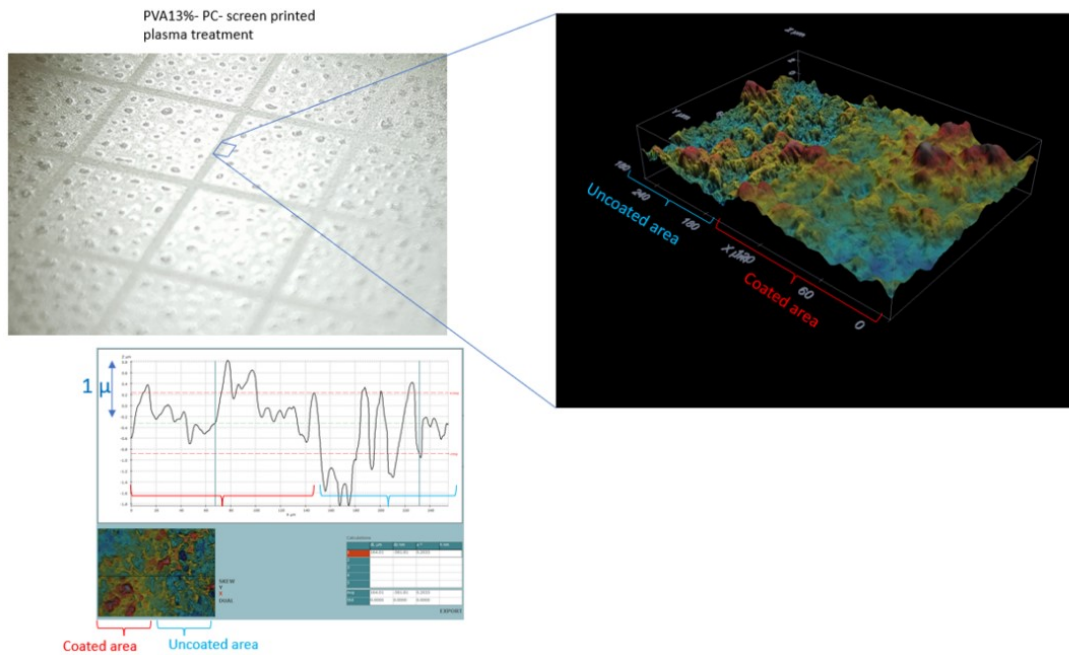


Figure S8. Bubble formation of screen-printed PVA. Photographs and 3D profile of 13% PVA printed on PC without surfactant (top). Micrographs of meander structures printed on PC using 13% PVA.

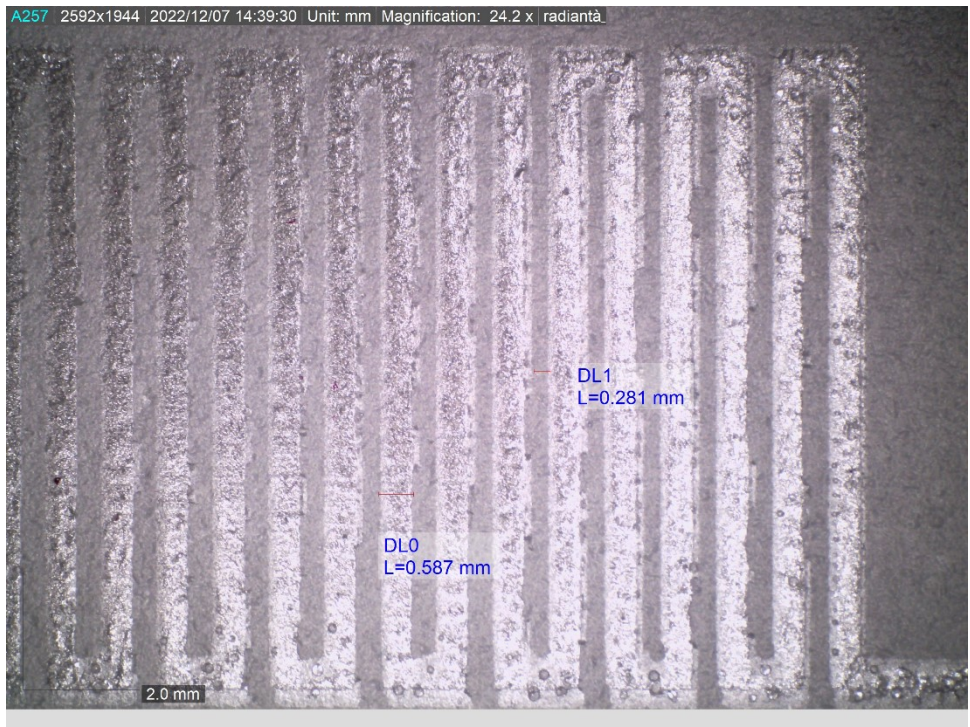


Figure S9. Suppressed bubble formation of screen-printed PVA. Mikrograph of three layers of 15% PVA with 10 mmol/kg printed on PC

SI 7. PVA dissolution

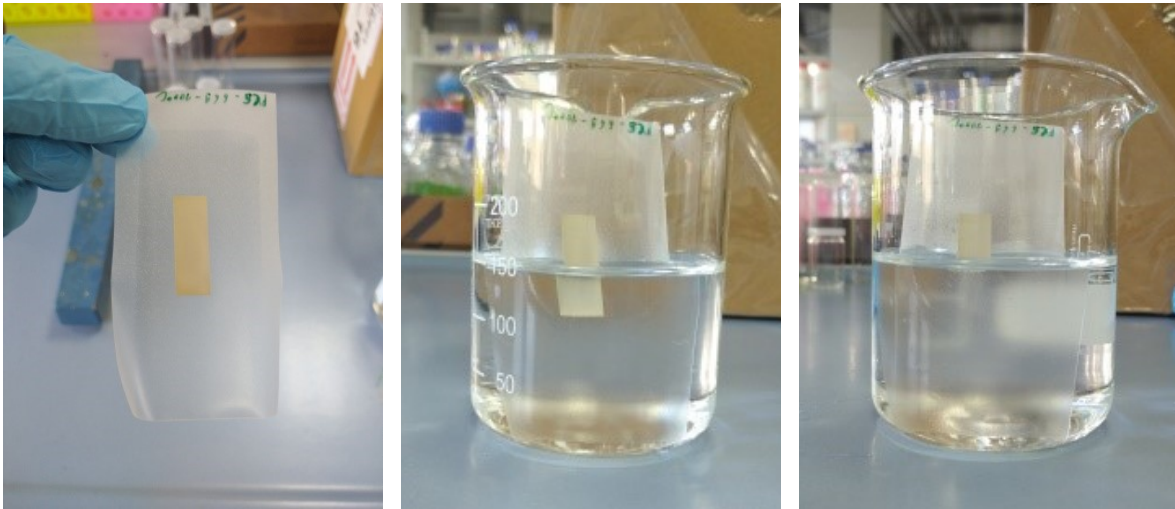


Figure S10. Dissolution of PVA. Photographs of wide silver tracks being released from PC foil by dissolution of the polymer.

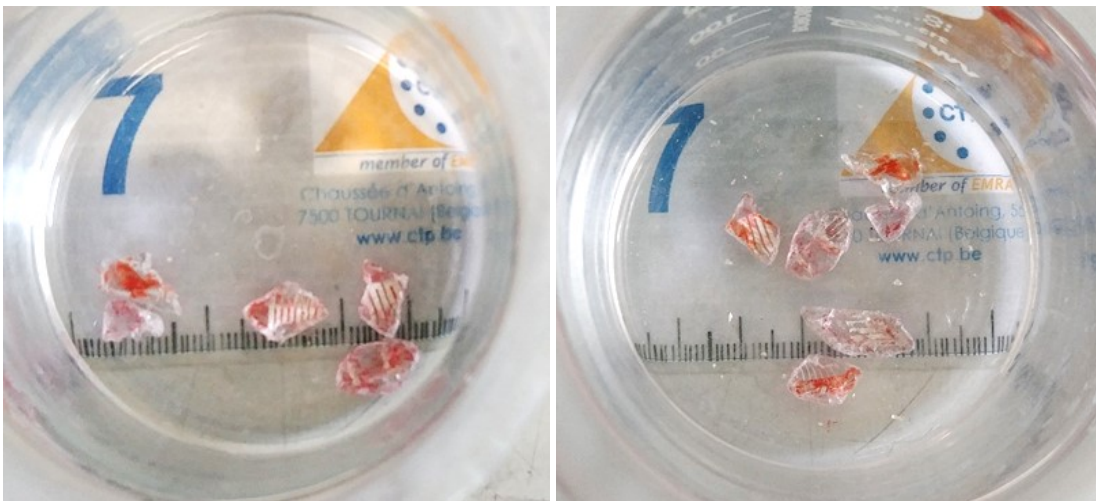


Figure S11. Separation of polymer and ink. Photographs sample type c). PC shreds with attached silver right after shredding (left). Partially separated polymer and silver particles after 30 minutes immersion in water (right).

SI 8. Silver recovery

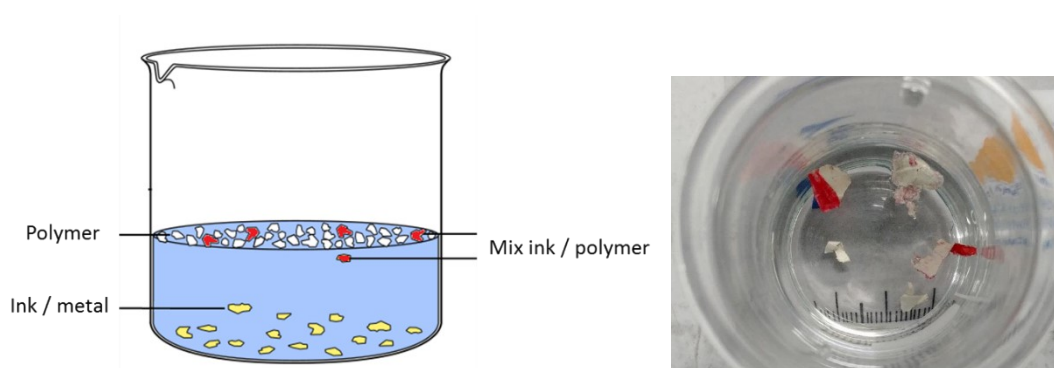


Figure S12. Dense media separation. Schematic (left) and photograph (right) of this method.

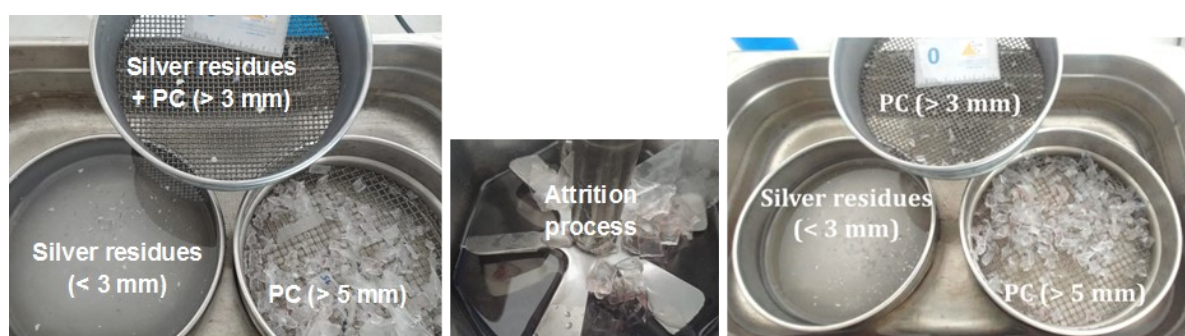


Figure S13. Silver and polymer segregation via sieving. Photographs of the wet screening process before attrition (left), after attrition (right), and the attrition step itself (middle).

Table S3. Silver recovery analysis. Recovery yield determined from loss on ignition (LOI) and ICP-OES measurements.

Test number	Mass (g)	Mass (%)	Grades		Recoveries	
			LOI (%)	Ag (%)	LOI (%)	Ag (%)
Test 18						
Oversized fraction (> 3 mm)	49	99.59%	99.97%	0.00036%*	99.6%	8.7%
Undersized fraction (< 3 mm)	0.2	0.41%	94.76%	0.91850%	0.4%	91.3%
Total	49.2	100.00%	99.94%	0.00409%	100.0%	100.0%

*0.00036%: Loss of material during analysis, value assumed from test 20.

Test number	Mass (g)	Mass (%)	Grades		Recoveries	
			LOI (%)	Ag (%)	LOI (%)	Ag (%)
Test 20						
Oversized fraction (> 3 mm)	48.9	99.29%	99.97%	0.00036%	99.3%	6.2%
Undersized fraction (< 3 mm)	0.35	0.71%	96.98%	0.75214%	0.7%	93.8%
Total	49.25	100.00%	99.95%	0.00570%	100.0%	100.0%

SI 9. Experimental observations

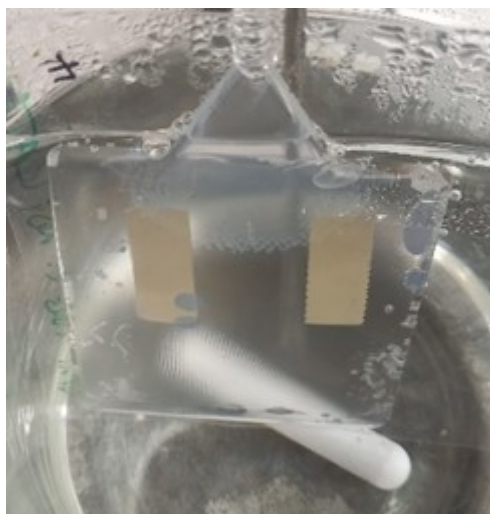


Figure S14. Direct dissolution test. Photograph of the samples with full PVA coating, overmold, and wide silver tracks (type d), pendent in hot water.

Table S4. Influence of milling on the recycling process and recovery of the ink.

Milling process	Shredding		Knife milling		Shredding +knife milling	
	A, D	B, C	A, D	B, C	A, D	B, C
Milling efficiency	Yes	Yes	No (mill blockages)		Yes	Yes
Delamination observed	Yes	Yes, but partial	Yes	Yes	Yes	Yes, but partial
Separation between ink and PC	Yes (dissolution)	Partial (sample C)	Yes (direct separation or dissolution)	Partial (without dissolution)	Yes (dissolution)	Partial (sample C)
Conclusion	Applicable	Not applicable (partial recovery)	Not applicable (milling blockages)		Applicable if fine milling required	Not applicable (partial recovery)